# Cell Design for the DARHT Linear Induction Accelerators

M. Burns, P. Allison, L. Earley, D. Liska, C. Mockler, J. Ruhe, H. Tucker, L. Walling
Los Alamos National Laboratory, P.O. Box 1663, Los Alamos, NM 87545

*Abstract*

The Dual-Axis Radiographic Hydrotest (DARHT) facility will employ two linear induction accelerators to produce intense, bremsstrahlung x-ray pulses for flash radiography. The accelerator cell design for a 3-kA, 16-20 MeV, 60-ns flattop, high-brightness electron beam is presented. The cell is optimized for high-voltage stand-off while also minimizing the its transverse impedance. Measurements of high-voltage and rf characteristics are summarized.

## I. INTRODUCTION

The DARHT facility at Los Alamos will generate intense bremsstrahlung x-ray pulses for radiography using two linear induction accelerators (LIA). Each LIA will produce a 3-kA, 16- to 20-MeV, 60-ns flattop, high-brightness electron beam using a 4-MeV injector and a series of 250-kV induction cells. Each cell consists of an oil-insulated ferrite core, an accelerating gap with carefully profiled electrodes and insulator, and a solenoid magnet to transport the electron beam. This paper summarizes the design of the accelerating gap region.

The cell development process included the design, fabrication, and testing of three prototype cell configurations. In chronological order, these are referred to as Mod 0, Mod 1, and Mod 2 and are shown in Fig. 1.

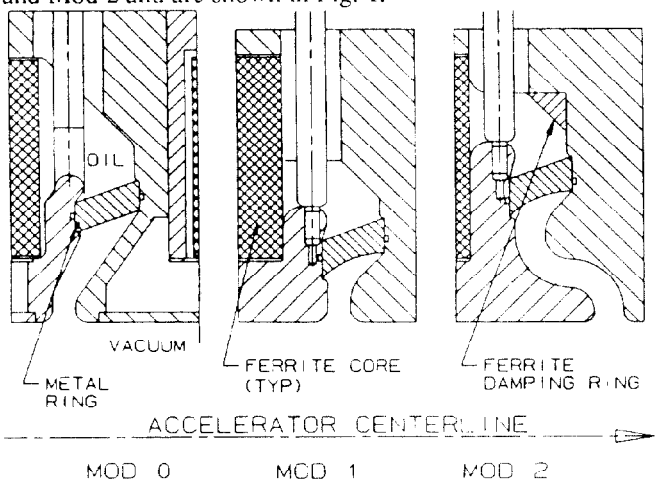


Fig. 1. Accelerating gap region of the three prototype DARHT cell designs.

The fundamental parameters of the accelerator determined the basic layout of each configuration. To provide the required pulse width while using readily available material, 11 TDK PE11B ferrite torroids (237 mm ID, 503 mm OD, 25.4 mm thick) were specified for the cell core. High-voltage breakdown of the accelerating gap is prevented by using a minimum gap width of 14.6 mm. The cell bore is 148.2 mm, which is a compromise between the large bore needed to limit growth of the beam breakup (BBU) instability and the small bore required to provide space for the solenoid magnet and to reduce costs.

The high-voltage design and breakdown measurements of these prototypes is discussed in Section 2. Section 3 deals with calculation and measurement of the transverse impedance of each configuration.

## II. HIGH-VOLTAGE DESIGN

We limited the peak design electric field stress to 200 kV/cm for the type 304 stainless steel electrodes that form the accelerating gap. This condition required a minimum gap width of 14.6 mm to sustain the 292-kV gap potential generated by the failure mode in which the cell is pulsed without electron beam loading.

The design of the insulator separating the oil-filled ferrite core from the vacuum portion of the cell became the focus of the high-voltage design. Empirical electrical breakdown formulas determined the initial layout of each insulator, and then detailed electric field modeling was carried out using the two-dimensional finite-element codes POISSON and FLUX2D. The breakdown electric field was maximized by optimizing the angle between the insulator and the calculated electric potential lines. This angle should be held near 40° for the cross-linked polystyrene insulator, and to do this in the Mod 0 design required placing a conducting ring within the insulator near the negative electrode vacuum triple point. The curved vacuum-side surface of the Mod 1 and Mod 2 insulators avoids the fabrication challenges encountered with the Mod 0 insulator ring. The maximum calculated electric field stress across the Mod 2 insulator was 93 kV/cm.

Cross-linked polystyrene (trade name Rexolite) was selected for the insulator because of its low dielectric constant ($\varepsilon$=2.5) and excellent mechanical properties. The insulator is compressed from 0 to 0.5 mm when installed to avoid small gaps between the electrodes and the insulator, which can cause significant field enhancement.

Interaction of the electron beam with the insulator may lead to insulator charging and UV-induced breakdown. The Mod 0 design counteract this effect by partially shielding the insulator from the electron beam. The Mod 1 design ignores this feature in favor of reduced machining costs. The Mod 2 design completely shields the insulator in a way that also reduces the design's transverse impedance. Detailed modeling of the complicated Mod 2 geometry required increasing the accelerating gap width to 19.1 mm.

L.M. Earley, *et. al.* [1], have completed detailed measurements of the breakdown voltage for each cell

Work performed under the auspices of the U.S. Department of Energy

0-7803-0135-8/91$01.00 ©IEEE

configuration. Mod 0 tests were carried out with two full-sized cells driven by a low-impedance (10 Ω) Blumlein. Full-sized Mod 1 and Mod 2 geometries were investigated using a higher impedance (240 Ω) cable pulser, which avoided the cost of fabricating the ferrite core portion of the cells. The Blumlein provided a square pulse with the voltage above 90% of the peak value for about 70 ns. The square waveform from the cable pulser remained above 90% of the peak for 150 ns.

Approximately 2000 shots were recorded in testing the Mod 0 design. These included conditioning shots at lower voltages as well as shots up to the breakdown voltage. In a similar way, the cable pulser was used for 30,000 shots on Mod 1 and roughly 4000 shots on Mod 2. The high-impedance cable pulser did not drive large currents when the gaps broke down, unlike the low-impedance Blumlein system. Thus, the cable pulser may have provided better high-voltage conditioning than the Blumlein system. The measured Mod 1 and Mod 2 breakdown voltages listed in Table 1 are the levels at which breakdown was observed for approximately half the shots at that potential. These breakdowns damaged the cells so that breakdown continued at -400 kV. No permanent damage was done to the electrodes or insulators, however, and these parts could be reused after cleaning. Mod 0 failed on the tenth shot at -350 kV, and testing was stopped at that point.

Table 1. Measured Breakdown Voltage

| Design | Breakdown (kV) | Driver |
|---|---|---|
| Mod 0 | -350 +/- 10% | Blumlein |
| Mod 1 | -500 +/- 8% | Cable pulser |
| Mod 2 | -520 +/- 8% | Cable pulser |

## III. CELL IMPEDANCE

The BBU instability results in high-frequency transverse oscillations of the electron beam, which smears the time-integrated beam spot size at the accelerator final focus. This increases the radiographic spot size and decreases the spatial resolution of the resulting radiograph. Growth of the BBU instability is dependent upon the cell transverse impedance.

Theory [2] indicates that :

$$\omega \left(\frac{c\,Z}{\omega}\right) = \frac{4w}{b^2}\,\eta\,, \qquad (1)$$

where Z is the transverse impedance (Ω/cm) of a resonant mode of angular frequency ω. The speed of light is c (cm/sec), the gap width is w (cm), and the bore radius is b (cm). η is a dimensionless constant that reflects how well the cavity modes are damped. Its value is determined by such factors as geometry and material choice. Minimizing the transverse impedance by minimizing η is the goal of the rf design of the cell.

The two-dimensional finite-difference, time-domain electromagnetic simulation code AMOS [3] was used to calculate the transverse impedance of the cell. This code is unique in that the rf absorption properties of the ferrite core are modeled. The ferrite properties were determined by measurements of small ferrite samples [4].

The low-impedance cell design process began with the Mod 0 configuration, which was an evolution of existing LIA designs. Mod 1 was a mechanical simplification of Mod 0 while also improving the cell's high voltage characteristics. Mod 2 used a "shielded gap" [5] to reduce the impedance at low frequency while also hiding the insulator from the electron beam. Our studies of these configurations with AMOS have shown that the transverse impedance can be reduced by using a low-dielectric-constant insulator material, placing the insulator close to the cell bore, avoiding gaps between the negative electrode and the ferrite core, matching rf waves into the core by controlling the amount of ferrite exposed to the cavity, using extra ferrite pieces to damp cavity modes, and properly choosing the geometry of the accelerating gap.

L. Walling, *et. al.* [6], have completed measurements of the transverse impedance of each cell design. These tests have shown that an important feature of the cell is the high-voltage drive rods attached to the negative electrode in two places 180° apart. The drive rods break the axial symmetry of the cell resulting in azimuthal variations in the impedance that cannot be modeled by AMOS. Figure 2 shows the transverse impedance measurement for the Mod 0 geometry in both the horizontal (parallel to the drive rods) and vertical (perpendicular to the drive rods) planes with the drive rods terminated in 30 Ω.

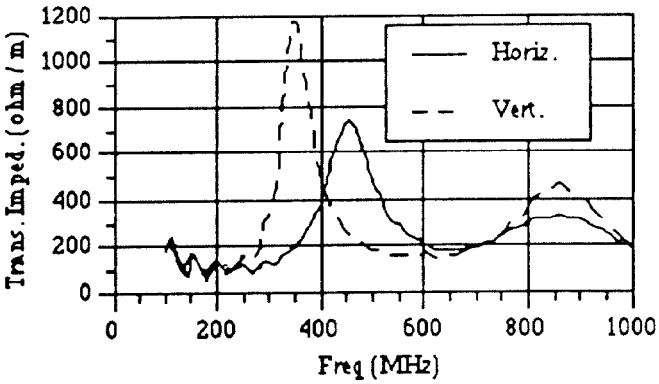


Fig. 2. Mod 0 transverse impedance in the horizontal and vertical planes.

P. Allison, *et. al.* [7], have shown that rotating pairs of cells 90° along the accelerator can take advantage of this mode splitting and reduce the effective impedance of the cell. With this installation pattern, the average of the horizontal and vertical impedances is the quantity of importance. This value should be roughly 670 Ω/m to meet the DARHT performance goals.

Figure 3 shows the average impedance vs frequency for all three cell configurations using the hollow compensation resistor discussed below. The small-amplitude oscillations in each curve are the result of calibration errors. The overall measurement accuracy is estimated to be better than 20%. The peak impedance for the Mod 0 design was 731 Ω/m at 114 MHz (η=2.29). The Mod 1 cell is much worse with a

measured peak impedance of 1275 Ω/m at 847 MHz (η=3.99). This is reduced in the Mod 2 design to 671 Ω/m at 816 MHz (η=1.61). The shielded-gap configuration has greatly reduced the magnitude of low-frequency modes. Without the damping ferrite (see Fig.1), however, measurements of the Mod 2 cell indicate that the high-frequency mode grows to 1020 Ω/m at 680 MHz.

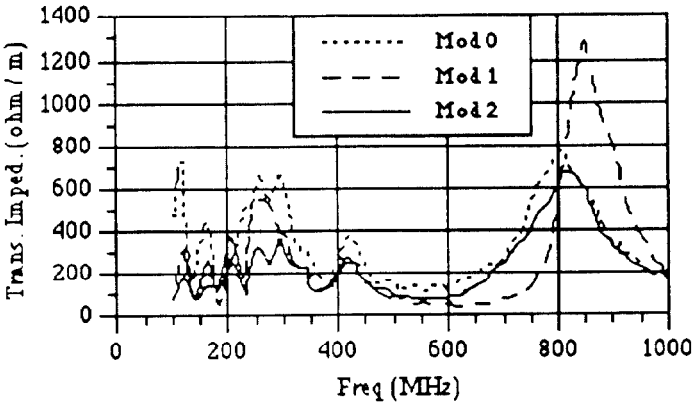


Fig. 3. Average transverse impedance vs frequency.

Attached to each side of the cell is an enclosure from which the drive rods enter the cell and in which is placed a compensation resistor. These resistors are electrically in parallel with the accelerating gap and help to reduce gap-voltage fluctuations due to electron-beam current variations.

The three enclosure/resistor designs shown in Fig. 4 were investigated in the belief that these assemblies may affect the cell impedance. In the first design, the high-voltage cable feeding the cell was connected directly to the drive rod, and a solid resistor ran along side the cable from the drive rod to ground. A hollow, cylindrical resistor was placed coaxially around the cable in the second enclosure. The third enclosure was designed to be similar to a high-power rf load. This design is referred to as the rf-horn because the resistor is surrounded by an exponential horn that maintains a constant impedance along the length of the resistor.

Shunt-resistance measurements of each enclosure design are shown in Fig. 5. The results clearly indicate that the rf-horn is the most successful design. Measurements of the accelerating cells with the various enclosures attached, however, indicate that the compensation resistor enclosure has very little effect on the transverse impedance of the cell. This result may be peculiar to the specific geometry of these designs.

## IV. Conclusions

We will construct a series of Mod 2 cells for system-level integrated tests of the DARHT accelerators. This design exhibited the best high-voltage and impedance properties. The shielded gap did not significantly reduce the peak impedance compared to Mod 0, but did allow complete shielding of the insulator from the electron beam and a larger accelerating gap.

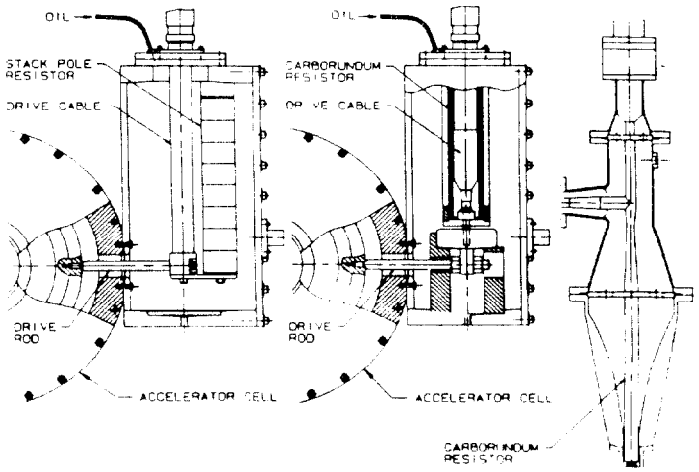


Fig. 4. Prototype compensation resistor enclosures

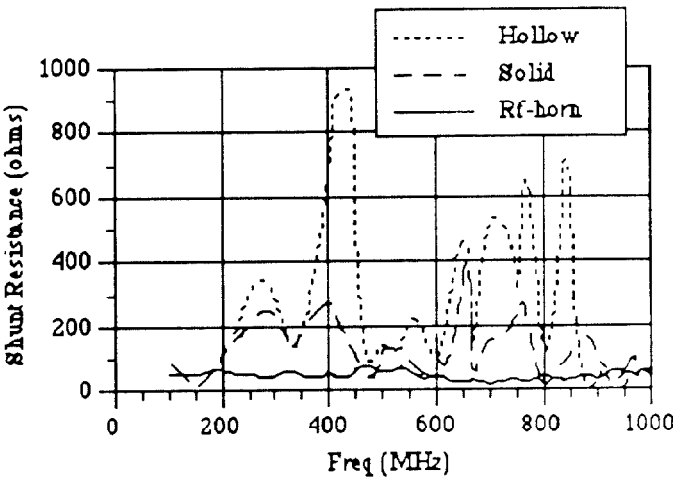


Fig. 5. Compensation resistor enclosure shunt resistance

## References


[1] L.M. Earley, "Induction Cell Insulator Experiments for the Dual-Axis Radiographic Hydrotest (DARHT) Facility", *IEEE Eigth Pulsed Power Conference*, San Diego, CA, June 1991.

[2] G.J. Caporaso and A.G. Cole, "Design of Long Induction Linacs", *1990 Linear Accelerator Conference*, Albuquerque, NM, Sept. 1990.

[3] J.F. DeFord, G.D. Craig, R.R. McLeod, "The AMOS Wakefield Code", *Workshop on Accelerator Computer Codes*, Los Alamos, NM, January 1990.

[4] J.F. DeFord and G. Kamin, "Application Of Linear Magnetic Loss Model of Ferrite to Induction Cavity Simulation", *1990 Linear Accelerator Conference*, Albuquerque, NM, Sept. 1990.

[5] R.B. Miller, B.M. Marder, P.D. Coleman, "The Effect of Accelerating Gap Geometry on the Beam Breakup Instability in Linear Induction Accelerators", J. Appl. Phys., 63 (4), Feb 1990, pp. 997-1008.

[6] L. Walling, P. Allison, M. Burns, D. Liska, D. McMurry, A. Shapiro, "Transverse Impedance Measurements of Prototype Cavities for a Dual-Axis Radiographic Hydrotest Facility (DARHT)", *IEEE 1991 Particle Accelerator Conference*, San Francisco, CA, May 1991.

[7] P. Allison, M. Burns, G. Caporaso, A. Cole, "Beam-Breakup Calculations for the DARHT Accelerator", *IEEE 1991 Particle Acclerator Conference*, San Francisco, CA, May 1991.